

Full Length Research Paper

Spectral sensitivity coefficients (SSCs) of the based materials for photonic devices under optical wavelength and temperature sensing variations in modern optical access networks

Abd El-Naser A. Mohammed, Ahmed Nabih Zaki Rashed* and Abd El-Fattah A. Saad

Electronics and Electrical Communication Engineering Department, Faculty of Electronic Engineering, Menouf 32951, Menoufia University, Egypt.

Accepted 21 August, 2009

In the present paper, the study of mathematical model of the spectral sensitivity coefficients of the based materials for photonic devices such as conventional and a thermal arrayed waveguide grating (AWG) against spectral optical signal wavelength and ambient temperature sensing variations within through three different fabrication materials based waveguides employed in conventional and a thermal (AWG) in modern local area passive optical access networks based on the Mathematical Laboratory (MATLAB) curve fitting program.

Key words: Optical access networks, conventional AWG, a thermal AWG, spectral sensitivity coefficients, local area network, planar optical waveguide, nonlinear optics.

INTRODUCTION

The optical access is gaining more interest as the demand for higher and higher bandwidth is getting stronger. The major drivers for larger bandwidth are the increasing processing power of user terminals and development of services that require substantially larger bandwidth than available in present day access networks. The prevailing access techniques (Hibino, 2002), such as the digital subscribes line systems and cable modems, are capable of supporting up to few tens of Mbit/s access rates per user, but the transport distance is limited. The optical access offers significantly higher bit rates and longer transport distances. The main sources of cost in running an existing network are the maintenance and powering of active network equipment. The idea of PON is to use passive components which have no components can be used for the purpose. The optical splitter/combiner is used with Time Division Multiplexed (TDM) PON networks. It divides the optical power, originating from the OLT, to all ONUs and combines the upstream signals

coming from the ONUs into a single fiber. In Wavelength Division Multiplexed (WDM) networks, Arrayed Waveguide Gratings (AWG) devices are used for the traffic distribution (Okamoto and Yamada, 1995). Planar light wave circuits (PLC) fabricated using silica-based waveguides are employed in various devices because of their excellent design flexibility, stability, and mass-producibility. Of the PLC-type devices, arrayed waveguide gratings (AWGs) are superior to other types of wavelength multi/demultiplexers, such as dielectric multi-layered filters, in the terms of compactness and multi-channeling. This is because multiple-interference makes it possible to form an AWG in a single device regardless of its channel count (Okamoto and Sugita, 1996). So, 16- to 64-channel AWGs have already been marketed and are widely used as multi/demultiplexers in DWDM systems employed in core networks in such areas as North America and Japan. At the same time, there is also a need for AWG multi/demultiplexers to be further improved in terms of channel count and made more compact and less expensive. Moreover, the functions and scale of PLCs should be enhanced to allow us to construct future photonic networks that need advanced optical processing such as optical switching and routing (Amersfoot et al.,

*Corresponding author. E-mail: ahmed_733@yahoo.com. Tel.: +2 048-3660-617. Fax: +2 048-3660-617

1996). Arrayed Waveguide Gratings (AWGs) have increasingly become more important in Wavelength Division Multiplexing (WDM) systems. The performance of wavelength division multiplexing (WDM) optical networks (Ho and Chen, 1997) greatly depends on the spectral characteristics of their components. One key component of WDM networks is the arrayed waveguide grating (AWG) (Noguchi et al., 2004), which can serve as a wavelength router, multiplexer, and demultiplexer. In order to allow the concatenation of many such devices and reduce the need for accurate wavelength control, their filter response must approximate a rectangular function. Various techniques have been proposed in order to broaden and flatten the transfer function of an AWG. The suppression of the spectral and temperature sensitivity of arrayed-waveguide grating (AWG) (de)multiplexers has been a subject of considerable interest in the last few years. This interest is driven primarily by closer channel spacing of systems based on dense wavelength-division multiplexing and the need for improved wavelength precision relative to the ITU standard grid. In pure silica-based AWGs, the channel peak wavelength shifts as a result of the temperature dependence of the refractive index of the waveguide. A common approach to eliminate the wavelength shift is to use an external heater or thermoelectric cooler maintaining the device at a constant temperature. However, this requires provision of electric power to an otherwise passive device, incorporation of temperature sensing and controlling elements, resulting in a complex package. Alternative solutions to produce temperature-insensitive AWGs have, thus, continued to be proposed. Among them, introduction of grooves placed at the center of the grating waveguides and filled with a material having an opposite refractive index temperature dependence than the glass waveguide, have been described (Parker and Walker, 1999). However, in this approach, grooves must be fabricated with high precision in order to avoid additional contributions to phase errors that degrade performance of AWGs. Another approach is to use the thermal expansion of a metal plate to displace the input coupler. This method, however, requires cutting the device in two parts, polishing all the surfaces, and precise realignment of the parts into a functional device (McGreer, 1998). The explosive growth of Internet traffic is pushing the rapid development of high-speed broadband optical networks, such as dense wavelength-division multiplexing (DWDM) systems. In these optical access advanced communication networks, a variety of optical components such as wavelength-division multi/demultiplexer (MUX/DEMUXs), Erbium-doped fiber amplifiers (EDFAs), lasers, photo detectors, and modulators are indispensable for constructing optical networks. Among others, arrayed waveguide grating (AWG)-type MUX/DEMUXs based on planar light wave circuits (PLCs) have played an important role as a key optical component for DWDM. Meanwhile, in the midst of the telecom winter, many carriers

are struggling to reduce per-bit cost. Therefore, optical components are expected to have new functions that reduce the operational and capital expenditures. For example, an AWG itself is expected to be a thermal as well as low cost. In order to lower the cost of AWGs, besides testing and packaging costs, chip size is quite important because the number of AWGs laid out over a wafer determines the general cost. This is especially true for large-size optical circuits such as AWGs. The increase in refractive index difference between core and cladding is a quite useful way to reduce chip size. So far, several types of high-contrast waveguides have been reported to have been achieved by using several material systems (Goodman, 1988), such as a semiconductor waveguide (Saito et al., 2003), SiON waveguide, Si-wire waveguides, and silica-based waveguide. Among these waveguides, the silica-based waveguide is suitable in the light of low propagation loss as well as high reliability. This paper describes the usefulness of high-contrast waveguides, such as those with 1.5 and 2.5% refractive index difference between core and cladding. From the practical point of view, however, when a high-contrast waveguide is used, the coupling loss between the waveguide and fiber that results from mode-field mismatch increases and this should be reduced. Up to the present, several schemes for mode transfer have been proposed (de Peralta et al., 2004). Avoiding the addition of further processes is desirable when applying these schemes in order to maintain low cost. In this paper, a novel mode transfer is presented. It needs no special process treatment and achieves low coupling loss. In addition to that combined high-contrast AWG waveguides with the thermal structure by introducing crescent trenches with an adhesive into the slab waveguide of an AWG. WDM transmission systems have been evolving from point-to-point transmission to next-generation reconfigurable add/drop (Ooba et al., 2000). In such a system, power equalization is extremely important in considering the signal-to-noise ratio. Power equalization should be performed automatically to reduce operational expenditure. For the purpose of providing an example of AWG application, this paper presents two types of power equalization modules: a dynamic gain equalizer (DGE) and a variable optical attenuator (VOA)-MUX/DEMUX that will play an important role for next-generation WDM access optical networks (Yong and Louzhen, 2003). The use of waveguide division multiplexing systems is increasing rapidly and, in these systems, arrayed-waveguide gratings (AWGs) play important roles as multiplexer/demultiplexers. They offer compactness, high stability, excellent optical characteristics, and mass reducibility. Until now, AWGs have been developed solely for telecommunication applications, so their wavelength range has been limited to 1.3 - 1.6 μm (Amersfoort et al., 1996). However, for novel applications such as sensors, they need AWGs with a shorter wavelength range, including the visible wavelength range. This is because many ma-

terials and analyses have specific characteristics at these wavelengths. Until now, only theoretical consideration has been given to AWGs operating in the visible wavelength range. One of the key advantages of AWGs is their ability to provide the fine wavelength resolution required for optical spectroscopic sensors designed to identify materials and analyzes. This arises from the design flexibility of the waveguide layout and enables us to obtain arbitrary spectroscopic characteristics by changing the path length difference between neighboring arrayed waveguides and the focal length of the slab optical arrayed waveguides (Kaneko et al., 2000).

CONVENTIONAL AWG IN OPTICAL ACCESS NETWORKS

The conventional arrayed waveguide grating (AWG) in local area optical access network has seen considerable development in the past few years, primarily in the development of devices for use as wavelength-division-multiplexed (WDM) channel demultiplexers and routers. In contrast, AWG devices have seen only limited use in time-domain applications (Kang et al., 2003). For example, mode-locked pulse inputs have been spectrally sliced to yield pulses in the tens of picoseconds range at the repetition rate of the mode-locked source laser, and super continuum sources have been sliced to yield multiple optical wavelengths for high-speed systems studies. Modified AWG devices have also been used for fast Fourier transform optical pulse shaping. Each input pulse to the AWG produces a burst of very high-repetition-rate pulses. In principle, if a high-repetition-rate short pulse source is used as the input, continuous, or quasi-continuous trains of very high-repetition-rate short pulses may be generated as in a rate-multiplication scheme. Furthermore, identical femto-second pulse bursts with slightly shifted center wavelength are obtained at different output channels of the AWG, very much like the direct space-to-time (DST) pulse shaper. The silica-based arrayed-waveguide grating (AWG) multi/demultiplexer is a key component for constructing dense wavelength-division-multiplexing systems (Kato et al., 2000). The advent of high-capacity all-optical transport networks relies on the ability to manage a large number of optical connections, that is, terminating or rerouting at the optical nodes. Implementing this function in an all-optical layer network requires versatile, reliable, and high-performance optical devices. The arrayed waveguide grating (AWG) has been recognized as a key component in modern optical communications due to its special frequency-space features. Moreover, the need of optical networks and optical subsystems modeling is of great interest, due to the time and cost savings that optical modeling software provide. Therefore, there's a need for accurate device modeling to include any degradation sources that, for instance, have direct impact in

network planning and dimensioning. Optical networks are widely used in modern communication systems. The use of optical devices with good characteristics such as wide bandwidth, compact size, high fabrication tolerance, stable output, polarization independence, low power loss, etc., is becoming more and more important. Arrayed waveguide gratings (AWGs) are the key devices for wavelength division multiplexers/demultiplexers and wavelength routers in backbone optical networks. In recent years, fiber-to-the-home has been built gradually, the use of cyclic AWG in any wavelength bands is paid attention to and studied for its expansibility (Okamoto et al., 1997). The fast and global spread of Internet and multimedia communications is accelerating the growth of optical communication networks. Research and commercial interests in optical networks based on wavelength division multiplexing (WDM) systems are rapidly increasing. WDM provides a new dimension for solving capacity and flexibility problems in the telecommunication network. It offers a huge transmission capacity and allows for novel network architectures that are more flexible than traditional networks. Typical optical network started from point-to-point WDM transmission systems, and now is evolving to the ring architecture various optical devices and components have been developed to realize WDM-based optical networks, and some of them have already been installed in the commercial communication system. Among them, key components are the wavelength multiplexer and demultiplexer, which work to combine and separate various frequency channels. Many principles have been proposed and reported for realization of multiplexers and demultiplexers (Kohtoku et al., 2000). It is worth mentioning that multiplexing and demultiplexing are essentially the same except the direction of light wave propagation. More discussion is usually focused on demultiplexing, which can be also applied to multiplexing due to the reciprocity of light wave beam propagation. In the following, several major types of demultiplexers will be described. The thin-film interference filter is composed of more than two Fabry-Perot (F-P) cavities separated by dielectric layers, and each cavity contains a multi-layer structure with more than 50 layers. Thin-film filters with different wavelengths are cascaded in series for demultiplexing. Each WDM signal passing through one filter is received by an output fiber with a focusing lens. The number of desired WDM channels determines the number of filters and lens as needed in the demultiplexing system. The phenomenon known as photosensitivity has been used to fabricate fiber Bragg gratings (FBG) and long-period gratings (LPG). The FBG can be combined either with a directional coupler according to the Mach-Zehnder interferometer structure, or with a circulator to form a functional unit that splits one wavelength signal from others. Furthermore, the demultiplexer can be constructed by cascading the functional units (Moerman et al., 1997). Again, the number of such units is dependent on the number of the WDM channels. The

MZ interferometer configuration can also be realized in planar light wave circuits (PLCs). PLCs are waveguide devices that integrate fiber-matched optical waveguides on silicon or glass substrate to provide an efficient means of interaction for the guided-wave optical signals. It is rather difficult to reduce the wavelength spacing and increase the port count, which cannot meet the demands for a large number of channels. Since early 1990, research interests are increasingly focused on the monolithic integrated wavelength demultiplexers. Two main types of monolithic integrated wavelength demultiplexers are distinguished, namely, reflection grating spectrometer devices and arrayed waveguide gratings. Both are imaging devices, i.e., they image the field of an input waveguide consisting of multiple wavelength signals onto an array of output waveguides, respectively. The arrayed waveguide grating-based demultiplexers have been demonstrated in SiO_2/Si . In grating-based demultiplexers, a vertically etched reflection grating provides the dispersive and focusing properties required for demultiplexing. They are usually operated at low order, offering typically more than 50 nm free spectral range (FSR) for the demultiplexing of a large number of wavelength channels (Kohotoku et al., 2002). However, the losses depend critically on the quality of the vertically etched reflection grating mirror. Chemically-assisted ion beam etching (CAIBE) or reactive ion etching (RIE) are usually employed to achieve the verticality and smoothness of the deeply etched grating facets. More recently, demultiplexers based on PLC-type arrayed waveguide gratings (AWG) have been extensively investigated. This is due to the fact that they are compatible with conventional waveguide technology, suitable for large-scale integration, more fabrication tolerant and better for mass production. They are usually operated at higher orders with smaller free spectral range compared to the grating-based optical multiplexers and demultiplexers. The arrayed-waveguide grating (AWG), also known as Dragone-Smit router or PHASAR, is an extremely versatile device that features and combines simultaneously unique periodic spatial and frequency properties and the possibility of integration on a chip. The AWG has been proposed for the implementation of multiple applications that embrace the fields of devices, systems, and optical access communication networks. Examples of these include the production of spectrum-sliced sources, dispersion compensation, wavelength division multiplexing (WDM) multiplexers and demultiplexers, tunable filters, wavelength routing, and optical processing. The range of application is very extensive, and the specific design requirements may differ substantially in terms of insertion losses and their spectral uniformity, frequency periodicity, channel bandwidth, cyclic nature, polarization sensitivity, and crosstalk. Therefore, it is essential to develop design procedures that can tackle efficiently the particular requirements of these applications while keeping a general and comprehensive nature. Clearly, the

way to accomplish the latter objective is to base the design procedure on an electromagnetic model for the AWG device capable of providing full amplitude and phase information of the input, output, and intermediate electrical fields. Data traffic originating in metropolitan and local areas is growing rapidly, and flexible, large-capacity, and transparent networks are required. In conventional systems, the electrical routing processing capability is creating a bottleneck preventing network capacity expansion. For a metropolitan area network (MAN) and local area network (LAN) system, network scalability is one of the most important requirements. A multiservice provision with different management policies should be co-implemented with a simple network topology. For local government systems, including private e-government networks, education, and information sharing for city residents, a secure multiservice provision is required that does not disturb other private networks. Wavelength-division-multiplexing (WDM) interconnection based on wavelength routing will become the key technology for realizing such networks. We have already developed a full-mesh WDM star-structure network (AWG-STAR) based on an arrayed-waveguide-grating (AWG) router with a management system. Widespread availability of broadband connectivity to end users and small business premises is driving the development of next-generation service offerings consuming more and more bandwidth. In addition to the large downstream bandwidth required by high-resolution video services, carriers are now seeing significant growth in upstream bandwidth requirements as peer-to-peer applications start to propagate. In order to continue to meet customer expectations, carriers need to deploy optical fiber technologies as close to the customer premise as possible, thus enabling them to deliver data rates in excess of 100 Mbit/s to and from the customer. Fiber-to-the-Home (FTTH) rollout recently has started in a large number of municipalities across North America, Europe and Asia. With the steadily increasing bandwidth demand, service providers and utilities have realized that driving fiber deeper into the access network and closer to the end user offers them a significant competitive advantage. The significant investment for extending fiber into the access network is often subsidized by local, state or national governments in order to fuel the local economy. While FTTH deployments are ideal from a bandwidth perspective, Fiber to-the-Building (FTTB) and Fiber-to-the-Curb (FTTC) are common pragmatic rollout scenarios being adopted by many carriers today. The last mile within a building or neighborhood is typically bridged utilizing VDSL technology, which utilizes the existing copper-wire infrastructure and provides services with up to 100 Mbit/s of bandwidth. In response to the steadily increasing demand for bandwidth and networking services for residential users as well as enterprise customers, passive optical networks (PONs) have emerged as a promising access technology that offers flexibility,

broad area coverage and cost-effective sharing of the expensive optical links compared with the conventional point-to-point (P2P) transport solutions. In addition, they inherently concentrate traffic and greatly reduce the number of input ports in the access multiplexer, both important for the cost-sensitive residential access market. Owing to these advantages, PONs have generated during the last decade substantial commercial activity also reflected in the study of several standardization bodies. Since the initial standardization of ATM-based PONs (APONs or alternatively named in ITU-T G.983.1 standard Broadband PONs-BPONs) newer standards support multi-gigabit rates and better adapt to the packet-based Internet applications. In January 2003, the GPON (Gigabit PON) standards were ratified by ITU-T and were included in the G.984.x series of ITU-T Recommendations. Driven by a closed group of worldwide system vendors and national telecom operators, they are designed to support a mix of TDM, ATM and packet-based services, reaching symmetrical transmission rates of up to 1.244 or 2.488 Gb/s (Kikuchi et al., 2004).

In the present study, we have been investigated and analyzed parametrically and numerically the spectral sensitivity coefficients (SSCs) of the photonic devices such as conventional and a thermal arrayed waveguide grating (AWG) based on the fabrication materials of its waveguides of pure silica, PMMA polymer, and lithium niobate materials under spectral optical wavelength and ambient temperature sensing variations for the applications in advanced and modern optical access networks. The basic model and equation analysis are based on the Sellmeier equation and MATLAB curve fitting program.

MODELING BASIS AND EQUATIONS ANALYSIS

Pure silica material

The Sellmeier equation of the refractive-index (n) of this waveguide as a function of optical signal wavelength variations is under the form of (Fleming, 1985):

$$n^2 = 1 + \frac{B_1 \lambda^2}{\lambda^2 - B_2^2} + \frac{B_3 \lambda^2}{\lambda^2 - B_4^2} + \frac{B_5 \lambda^2}{\lambda^2 - B_6^2} \quad (1)$$

Where λ is the optical wavelength (μm), where the Sellmeier equation coefficients are as (Fleming, 1985): $B_1 = 10.668422193$, $B_2 = 0.0301516485 * (T/T_0)^2$, $B_3 = 3.043474218 * 10^{-3}$, $B_4 = 1.1347511235 * (T/T_0)^2$, $B_5 = 1.54133408$, $B_6 = 1.104 * 10^3$. T is the temperature of the material, K, and T_0 is the reference temperature and is taken as (300 K).

Then the differentiation of Equation (1) w. r. t. wavelength (λ) gives as follows:

$$2n \frac{\partial n}{\partial \lambda} = \frac{\partial}{\partial \lambda} \left[\frac{B_1 B_2^2}{\lambda^2 - B_2^2} + \frac{B_3 B_4^2}{\lambda^2 - B_4^2} + \frac{B_5 B_6^2}{\lambda^2 - B_6^2} \right] \quad (2)$$

Or

$$\frac{\partial n}{\partial \lambda} = -(\lambda/n) \left[\frac{B_1 B_2^2}{(\lambda^2 - B_2^2)^2} + \frac{B_3 B_4^2}{(\lambda^2 - B_4^2)^2} + \frac{B_5 B_6^2}{(\lambda^2 - B_6^2)^2} \right] \quad (3)$$

Then the complete differentiation w. r. t. λ gives as follows:

$$\frac{dn}{d\lambda} = -(\lambda/n) \left[\frac{1.05 B_1 B_2^2}{(\lambda^2 - B_2^2)^2} + \frac{0.9765 B_3 B_4^2}{(\lambda^2 - B_4^2)^2} \right] \quad (4)$$

PMMA polymer material

The Sellmeier equation of the refractive-index as a function of wavelength is under the form (Ishigure et al., 1996):

$$n^2 = 1 + \frac{C_1 \lambda^2}{\lambda^2 - C_2^2} + \frac{C_3 \lambda^2}{\lambda^2 - C_4^2} + \frac{C_5 \lambda^2}{\lambda^2 - C_6^2} \quad (5)$$

Where λ is in μm , the Sellmeier equation coefficients of Equation (5) are as the values (Ishigure et al., 1996):

$$C_1 = 0.4963, C_2 = 71.80 * 10^{-3}, C_3 = 0.6965, C_4 = 117.4 * 10^{-3}, C_5 = 0.3223, \text{ and } C_6 = 9237 * 10^{-3}.$$

Also, the differentiation of Equation (5) w. r. t. Wavelength (λ) gives following expression:

$$2n \frac{\partial n}{\partial \lambda} = \frac{\partial}{\partial \lambda} \left[\frac{C_1 C_2^2}{\lambda^2 - C_2^2} + \frac{C_3 C_4^2}{\lambda^2 - C_4^2} + \frac{C_5 C_6^2}{\lambda^2 - C_6^2} \right] \quad (6)$$

Or

$$\frac{\partial n}{\partial \lambda} = -(\lambda/n) \left[\frac{C_1 C_2^2}{(\lambda^2 - C_2^2)^2} + \frac{C_3 C_4^2}{(\lambda^2 - C_4^2)^2} + \frac{C_5 C_6^2}{(\lambda^2 - C_6^2)^2} \right] \quad (7)$$

Then the complete differentiation of Equation (5) w. r. t. λ gives the following expression:

$$\frac{dn}{d\lambda} = -(\lambda/n) \left[\frac{3.654 C_1 C_2^2}{(\lambda^2 - C_2^2)^2} + \frac{0.0943 C_3 C_4^2}{(\lambda^2 - C_4^2)^2} \right] \quad (8)$$

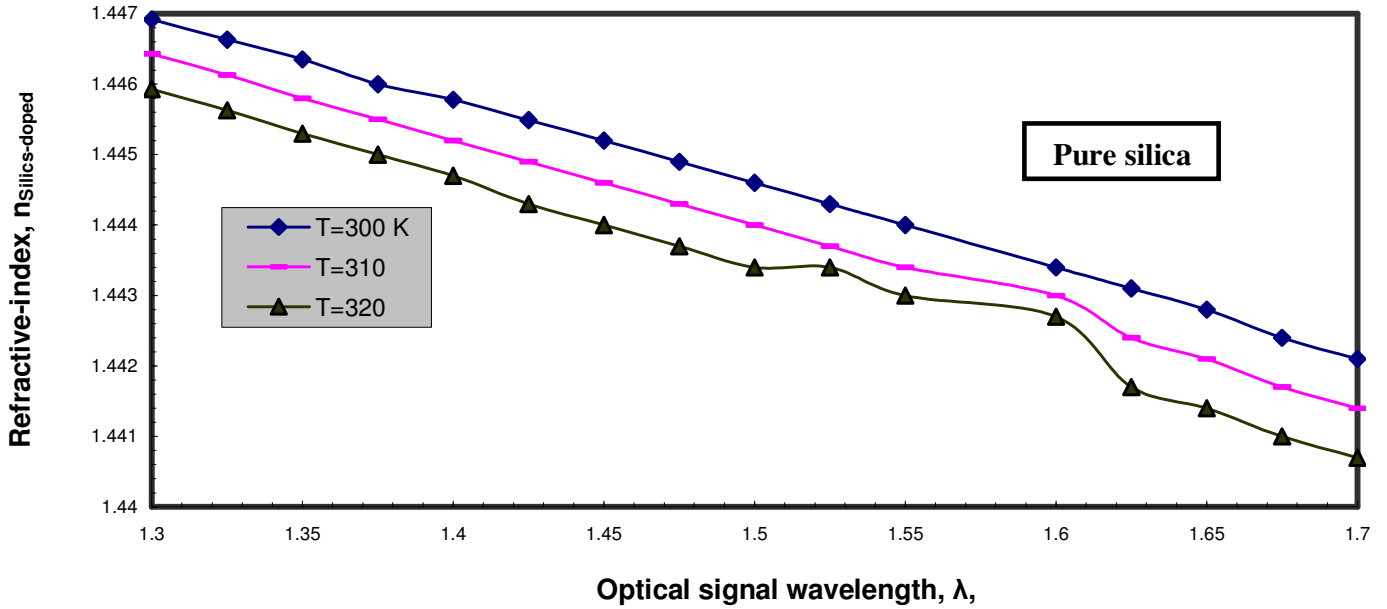


Figure 1. Variation of refractive-index (n) versus wavelength for pure silica material.

LiNbO₃ material

The Sellmeier equation of the refractive-index as a function of wavelength is under the form (Jundt, 1997):

$$n^2 = A_1 + A_2F + \frac{A_3 + A_4F}{\lambda^2 - (A_5 + A_6F)^2} + \frac{A_7 + A_8F}{\lambda^2 - A_9^2} - A_{10}\lambda^2 \tag{9}$$

Where λ is in μm and $F = T^2 - T_0^2$. T is the temperature of the material, K, and T_0 is the reference temperature and is considered 300 K. The set of parameters is recast and dimensionally adjusted as below [25]: $A_1 = 5.35583$, $A_2 = 4.629 \times 10^{-7}$, $A_3 = 0.100473$, $A_4 = 3.862 \times 10^{-8}$, $A_5 = 0.20692$, $A_6 = -0.89 \times 10^{-8}$, $A_7 = 100$, $A_8 = 2.657 \times 10^{-5}$, $A_9 = 11.34927$ and $A_{10} = 0.015334$.

Equation (9) can be simplified as the following expression:

$$n^2 = A_{12} + \frac{A_{34}}{\lambda^2 - A_{56}^2} + \frac{A_{78}}{\lambda^2 - A_9^2} - A_{10}\lambda^2 \tag{10}$$

$$A_{12} = A_1 + A_2F, A_{34} = A_3 + A_4F, A_{56} = A_5 + A_6F, A_{78} = A_7 + A_8F.$$

Also, the differentiation of Equation (10) w. r. t. Wavelength (λ) gives the following expression:

$$\frac{\partial n}{\partial \lambda} = \left(\frac{-\lambda}{n} \right) \left[\frac{A_{34}}{(\lambda^2 - A_{56}^2)^2} + \frac{A_{78}}{(\lambda^2 - A_9^2)^2} + A_{10} \right] \tag{11}$$

Then the complete differentiation of Equation (10) w. r. t λ gives the following expression:

$$\frac{dn}{d\lambda} = \left(\frac{-0.543 \lambda}{n} \right) \left[\frac{1.064 A_{34}}{(\lambda^2 - A_{56}^2)^2} + \frac{1.2765 A_{78}}{(\lambda^2 - A_9^2)^2} + 2.874 A_{10} \right] \tag{12}$$

ANALYSIS OF THE RESULTS

As shown in Figures (1 - 3) indicate that:

1) As the wavelength of waveguide material (λ) increases, refractive-index of the material (n) decreases in the three fabrication materials for waveguide at the constant temperature (T).

The refractive-index of Pure silica material is the lowest than the other materials (PMMA, LiNbO₃), so that the speed of light through the waveguide which is fabricated from Pure silica material is the highest than the other fabrication materials based on the fact that $(n=c/v)$, where v is the speed of light in the medium (waveguide). Then the low the refractive-index of the material, the high the speed of the light through its waveguide.

2) As shown in Figure 4, we can fit the relation between the variations of the refractive-index w. r. t the variation of wavelength ($dn/d\lambda$) as a function of three terms based on MATLAB curve-fitting program (Fleming, 1985):

$$\frac{dn}{d\lambda} = a_0 + a_1 T + a_2 T^2 \tag{13}$$

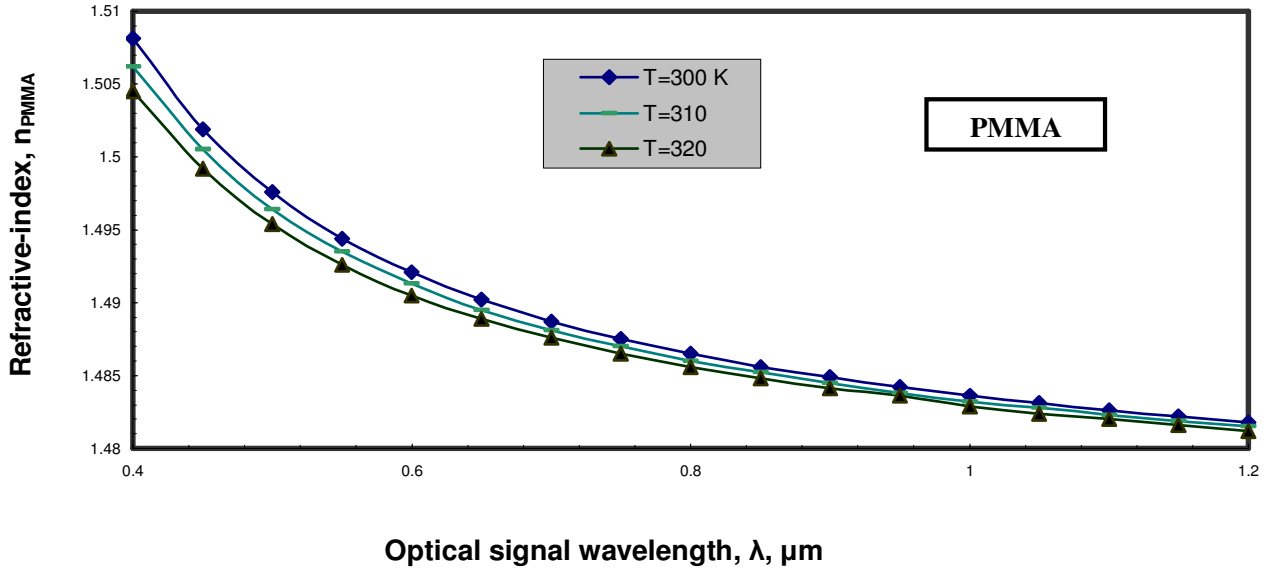


Figure 2. Variation of refractive-index (n) versus wavelength for PMMA material.

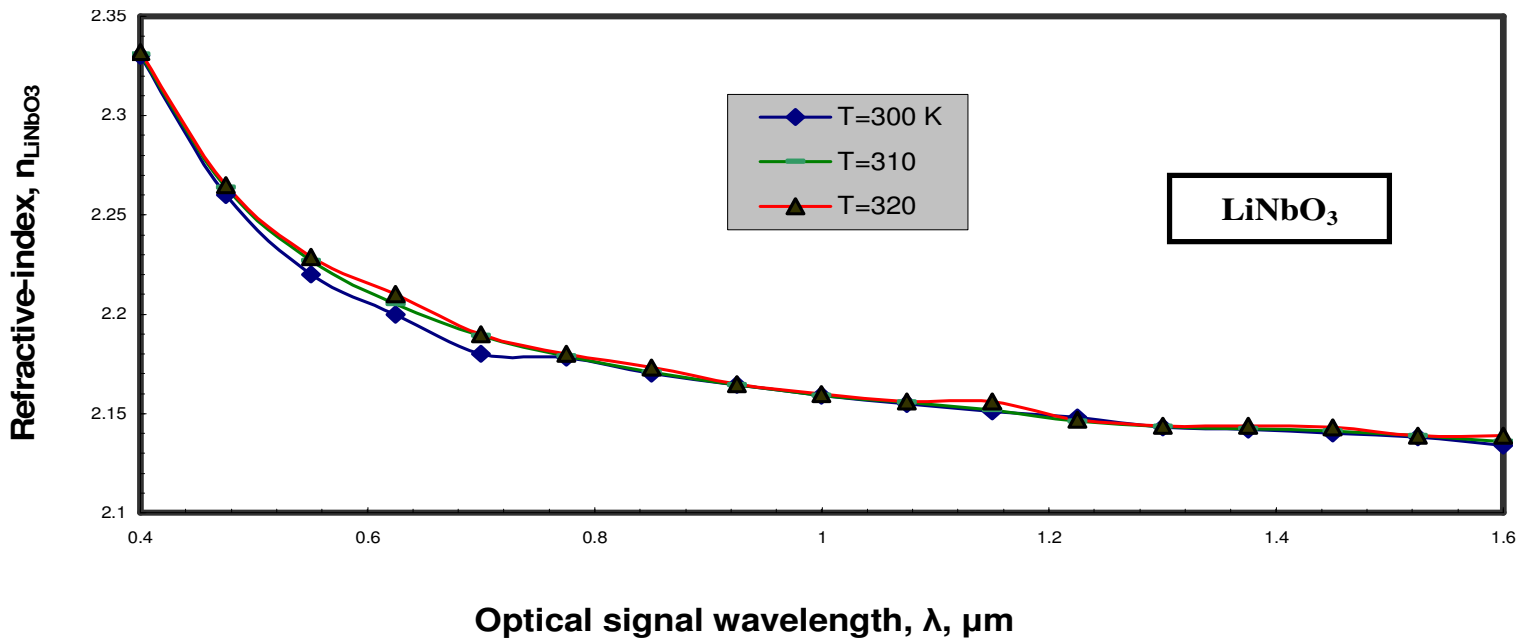


Figure 3. Variation of refractive-index (n) versus wavelength for LiNbO₃ material.

The fitting based on no. of 21 points iteration (300 K-320 K) at the starting wavelength (1.3 μm), with step-size variation of (0.1 μm), and the ending wavelength (1.7 μm) for the Pure silica material [see Appendix A]. Then we can fit the sensitivity coefficients (a_0, a_1, a_2) as a function of wavelength (λ).

$$a_0 = 19.64 - 27.3\lambda + 9.7\lambda^2 \quad (14)$$

$$a_1 = 0.26 - 0.32\lambda + 0.95\lambda^2 \quad (15)$$

$$a_2 = 0.2 - 28 \times 10^{-3} \lambda + 1 \times 10^{-4} \lambda^2 \quad (16)$$

Then the variation of the refractive-index w. r. t variation of wavelength ($dn/d\lambda$) in the form:

$$\frac{dn}{d\lambda} = \begin{bmatrix} a_0 & a_1 & a_2 \\ T \\ T^2 \end{bmatrix} \quad (17)$$

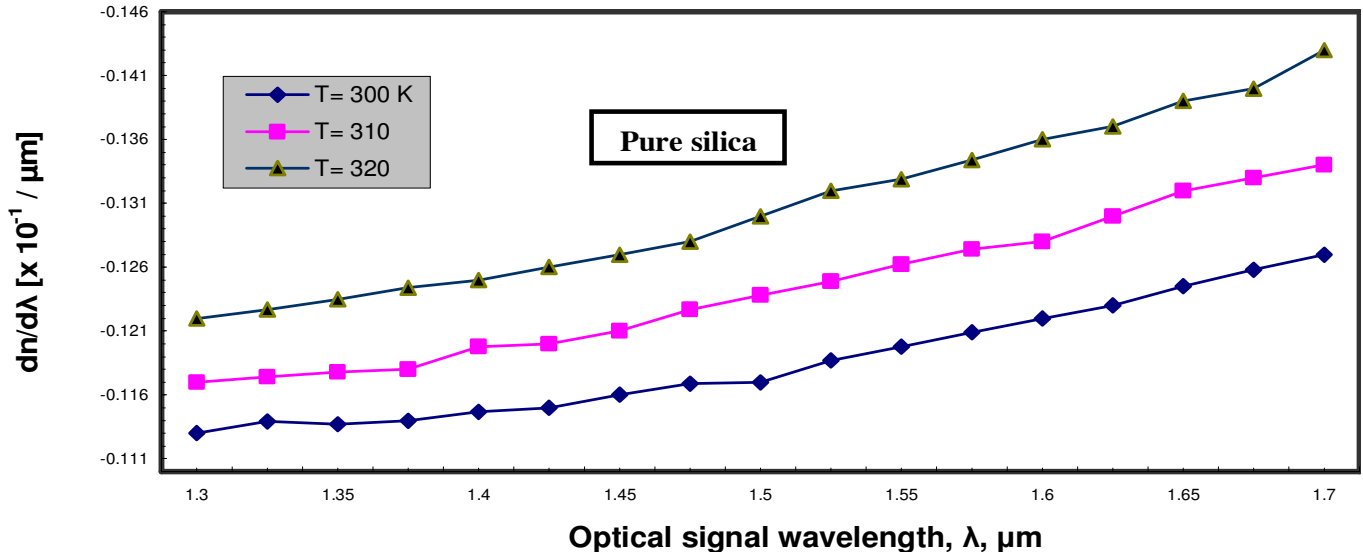


Figure 4. Variation of $dn/d\lambda$ versus wavelength for pure silica material.

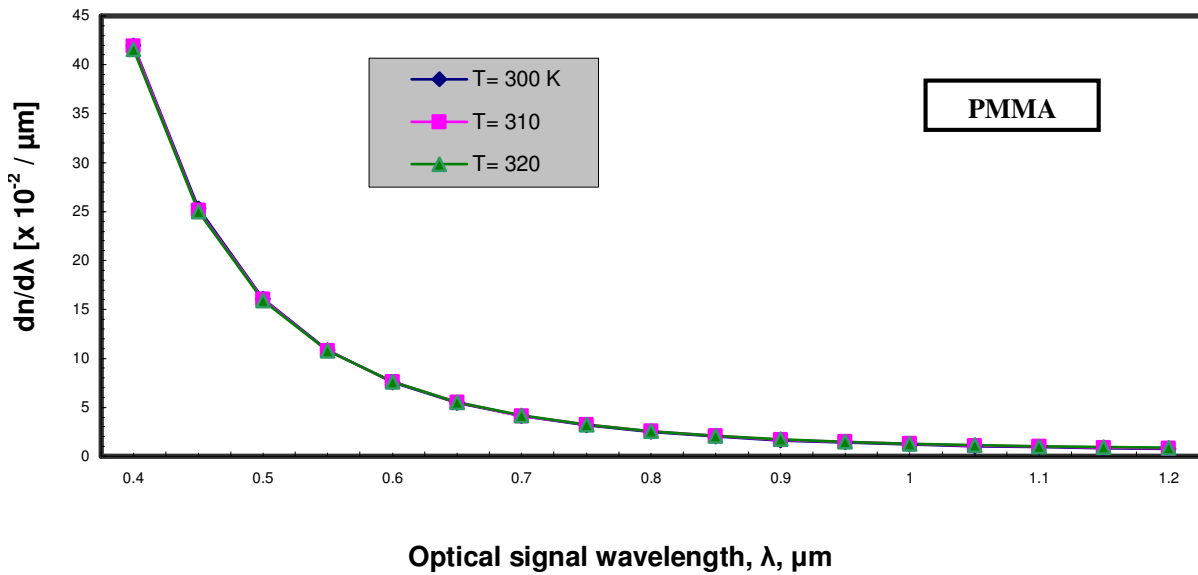


Figure 5. Variation of $dn/d\lambda$ versus wavelength for PMMA material.

In fact, the spectral sensitivity is given:

$S_{\lambda}^n = \alpha \left| \frac{dn}{d\lambda} \right|$, $\alpha = \frac{\lambda}{n}$, and as shown in Figures (1 and 4), as wavelength of the material (λ) increases, then the refractive-index of material (n) decreases, ($dn/d\lambda$) increases, and α also increases, this achieve very high Spectral Sensitivity for Pure silica material.

3) As shown in Figure 5, we can fit the relation between the variations of the refractive-index w. r. t the variation of wavelength ($dn/d\lambda$) as a function of three terms based on MATLAB curve-fitting program (Fleming, 1985):

$$\frac{dn}{d\lambda} = b_0 + b_1 T + b_2 T^2 \tag{18}$$

The fitting based on no. of 21 points iteration (300 K-320 K) at the starting wavelength (0.4 μm), with step-size variation of (0.2 μm), and the ending wavelength (1.2 μm) for the PMMA Polymer material [see Appendix B], also we can fit the sensitivity coefficients (b_0, b_1, b_2) as a function of wavelength (λ).

$$b_0 = 96.24 - 210.9\lambda + 105.62\lambda^2 \tag{19}$$

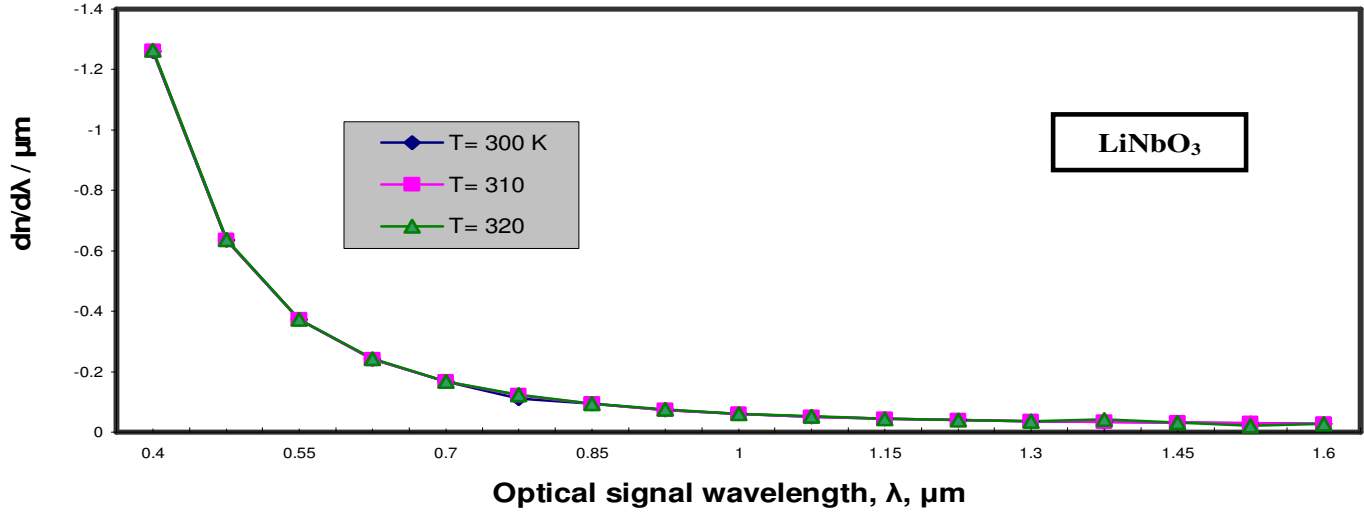


Figure 6. Variation of $dn/d\lambda$ versus wavelength for LiNbO_3 material.

$$b_1 = -0.6 - 1.34\lambda - 0.67\lambda^2 \quad (20)$$

$$b_2 = 0.98 \times 10^{-3} - 0.22 \times 10^{-2} \lambda + 1 \times 10^{-3} \lambda^2 \quad (21)$$

Then the variation of the refractive-index w. r. t variation of wavelength ($dn/d\lambda$) in the form:

$$\frac{dn}{d\lambda} = [b_0 \quad b_1 \quad b_2] \begin{bmatrix} 1 \\ T \\ T^2 \end{bmatrix} \quad (22)$$

In fact, the spectral sensitivity is given:

$$S_{\lambda}^n = \beta \left| \frac{dn}{d\lambda} \right|, \quad \beta = \frac{\lambda}{n}$$

and as shown in Figures (2 and 5), as wavelength of the material (λ) increases, then the refractive-index of material (n) decreases, ($dn/d\lambda$) decreases, and this achieve low Spectral Sensitivity for PMMA Polymer material.

4) As shown in Figure 6, we can fit the relation between the variations of the refractive-index w. r. t the variation of wavelength ($dn/d\lambda$) as a function of three terms based on MATLAB curve-fitting program (Fleming, 1985):

$$\frac{dn}{d\lambda} = c_0 + c_1 T + c_2 T^2 \quad (23)$$

The fitting based on no. of 21 points iteration (300 K-320 K) at the starting wavelength (0.4 μm), with step-size variation of (0.3 μm), and the ending wavelength (1.6 μm)

for the LiNbO_3 material [see Appendix C], we can fit the sensitivity coefficients (c_0, c_1, c_2) as a function of wavelength (λ).

$$c_0 = 12.45 - 21\lambda + 8.76\lambda^2 \quad (24)$$

$$c_1 = -0.97 + 0.16\lambda - 0.067\lambda^2 \quad (25)$$

$$c_2 = 0.16 \times 10^{-3} - 0.3\lambda + 0.12 \times 10^{-3} \lambda^2 \quad (26)$$

Then the variation of the refractive-index w. r. t variation of wavelength ($dn/d\lambda$) in the form:

$$\frac{dn}{d\lambda} = [c_0 \quad c_1 \quad c_2] \begin{bmatrix} 1 \\ T \\ T^2 \end{bmatrix} \quad (27)$$

In fact, the spectral sensitivity is given:

$$S_{\lambda}^n = \gamma \left| \frac{dn}{d\lambda} \right|, \quad \gamma = \frac{\lambda}{n}$$

and as shown in Figures (3 and 6), as wavelength of the material (λ) increases, then the refractive-index of material (n) decreases, ($dn/d\lambda$) decreases, and this achieve low Spectral Sensitivity for LiNbO_3 material.

Conclusions

In a summary, we have investigated and analyzed the basic mathematical model equations of the three fabrication materials based conventional and a thermal arrayed waveguide grating in local area passive optical access

networks under the assuming set of the controlling parameters of the ambient temperatures in the range of 300 K-320 K for the three fabrication materials. We have demonstrated that pure silica material has the highest spectral sensitivity coefficients, and moreover pure silica has low propagation loss of the light rays, and high reliability than the two fabrication materials such as PMMA and LiNbO₃ for conventional and a thermal AWG applications in passive optical access networks.

APPENDIX: A

We can fit the relation between the variations of the refractive-index w. r. t the variation of wavelength ($dn/d\lambda$) as a function of three terms based on MATLAB curve-fitting program (Fleming, 1985):

$$\frac{dn}{d\lambda} = a_0 + a_1 T + a_2 T^2 \quad (A1)$$

The fitting based on no. of 21 points (300 K-320 K) at the

Table 1. Pure silica material coefficients.

λ (μm)	a_0	a_1	a_2
1.3	0.85	-0.552×10^{-2}	0.885×10^{-5}
1.4	0.1	-0.674×10^{-3}	0.1×10^{-5}
1.5	-0.25	0.16×10^{-2}	-0.27×10^{-5}
1.6	2.18	0.014	0.226×10^{-4}
1.7	0.72	-0.46×10^{-2}	0.73×10^{-5}

starting wavelength (1.3 μm):

$$\frac{dn}{d\lambda} = 0.85 - 0.552 \times 10^{-2} T + 0.885 \times 10^{-5} T^2 \quad (A2)$$

The fitting based on no. of 21 points (300 K-320 K) at the wavelength (1.4 μm):

$$\frac{dn}{d\lambda} = 0.1 - 0.674 \times 10^{-3} T + 0.1 \times 10^{-5} T^2 \quad (A3)$$

The fitting based on no. of 21 points (300 K-320 K) at the wavelength (1.5 μm):

$$\frac{dn}{d\lambda} = -0.25 + 0.16 \times 10^{-2} T - 0.27 \times 10^{-5} T^2 \quad (A4)$$

The fitting based on no. of 21 points (300 K-320 K) at the wavelength (1.6 μm):

$$\frac{dn}{d\lambda} = 2.18 - 0.014 T + 0.226 \times 10^{-4} T^2 \quad (A5)$$

The fitting based on no. of 21 points (300 K-320 K) at the ending wavelength (1.7 μm):

$$\frac{dn}{d\lambda} = 0.72 - 0.46 \times 10^{-2} T + 0.73 \times 10^{-5} T^2 \quad (A6)$$

The Root Mean Square (r. m. s) for these fitting equations is approximately (0.013 %). The coefficients with the operating wavelength of silica as shown in Table (1).

Then the fitting the values in the Table (1) to indicate the coefficients (a_0, a_1, a_2) as a function of optical signal wavelength as follows:

$$a_0 = 19.64 - 27.3\lambda + 9.7\lambda^2 \quad (A7)$$

$$a_1 = 0.26 - 0.32\lambda + 0.95\lambda^2 \quad (A8)$$

$$a_2 = 0.2 - 28 \times 10^{-3} \lambda + 1 \times 10^{-4} \lambda^2 \quad (A9)$$

APPENDIX: B

We can fit the relation between the variations of the refractive-index w. r. t the variation of wavelength ($dn/d\lambda$) as a function of three terms based on MARLAB curve-fitting program (Fleming, 1985):

$$\frac{dn}{d\lambda} = b_0 + b_1 T + b_2 T^2 \quad (B1)$$

The fitting based on no. of 21 points (300 K-320 K) at the starting wavelength (0.4 μm):

$$\frac{dn}{d\lambda} = 34.54 - 0.22 T + 0.35 \times 10^{-3} T^2 \quad (B2)$$

The fitting based on no. of 21 points (300 K-320 K) at the wavelength (0.6 μm):

$$\frac{dn}{d\lambda} = -5.1 + 0.33 T - 0.53 \times 10^{-4} T^2 \quad (B3)$$

The fitting based on no. of 21 points (300 K-320 K) at the wavelength (0.8 μm):

$$\frac{dn}{d\lambda} = -1.05 + 0.7 \times 10^{-2} T - 0.11 \times 10^{-4} T^2 \quad (\text{B4})$$

The fitting based on no. of 21 points (300 K-320 K) at the wavelength (1 μm):

$$\frac{dn}{d\lambda} = -1.34 + 0.87 \times 10^{-2} T - 0.14 \times 10^{-4} T^2 \quad (\text{B5})$$

The fitting based on no. of 21 points (300 K-320 K) at the ending wavelength (1.2 μm):

$$\frac{dn}{d\lambda} = -9.2 - 0.06T - 0.95 \times 10^{-4} T^2 \quad (\text{B6})$$

R. M. S for these fitting equations is approximately (0.048%). The values of the coefficients with the operating wavelength of PMMA in Table (2).

Table 2. PMMA material coefficients.

λ (μm)	b_0	b_1	b_2
0.4	34	-0.22	0.35×10^{-5}
0.6	-5.1	0.033	-0.53×10^{-4}
0.8	-1.05	0.7×10^{-2}	-0.11×10^{-4}
1	-1.34	0.87×10^{-2}	-0.14×10^{-4}
1.2	-9.2	0.06	-0.95×10^{-4}

Table 3. LiNbO₃ material coefficients.

λ (μm)	c_0	c_1	c_2
0.4	5.9	-0.045	0.74×10^{-4}
0.7	1.39	-0.01	0.16×10^{-4}
1	-0.7	0.44×10^{-2}	-0.72×10^{-5}
1.3	1.7	-0.01	0.18×10^{-5}
1.6	0.43	-0.3×10^{-2}	0.47×10^{-5}

Then the fitting the values in the Table (2) to indicate the coefficients (b_0, b_1, b_2) as a function of optical signal wavelength as follows:

$$b_0 = 96.24 - 210.9\lambda + 105.62\lambda^2 \quad (\text{B7})$$

$$b_1 = -0.6 - 1.34\lambda - 0.67\lambda^2 \quad (\text{B8})$$

$$b_2 = 0.98 \times 10^{-3} - 0.22 \times 10^{-2} \lambda + 1 \times 10^{-3} \lambda^2 \quad (\text{B9})$$

APPENDIX: C

We can fit the relation between the variations of the refractive-index w. r. t the variation of wavelength ($dn/d\lambda$) as a function of three terms based on MATLAB curve-fitting program (Fleming, 1985):

$$\frac{dn}{d\lambda} = c_0 + c_1 T + c_2 T^2 \quad (\text{C1})$$

The fitting based on no. of 21 points (300 K-320 K) at the starting wavelength (0.4 μm):

$$\frac{dn}{d\lambda} = 5.9 - 0.045T + 0.74 \times 10^{-4} T^2 \quad (\text{C2})$$

The fitting based on no. of 21 points (300 K-320 K) at the wavelength (0.7 μm):

$$\frac{dn}{d\lambda} = 1.39 - 0.01T + 0.16 \times 10^{-4} T^2 \quad (\text{C3})$$

The fitting based on no. of 21 points (300 K-320 K) at the wavelength (1 μm):

$$\frac{dn}{d\lambda} = -0.7 + 0.44 \times 10^{-2} T + 0.72 \times 10^{-5} T^2 \quad (\text{C4})$$

The fitting based on no. of 21 points (300 K-320 K) at the wavelength (1.3 μm):

$$\frac{dn}{d\lambda} = 1.7 - 0.01T + 0.18 \times 10^{-5} T^2 \quad (\text{C5})$$

The fitting based on no. of 21 points (300 K-320 K) at the ending wavelength (1.6 μm):

$$\frac{dn}{d\lambda} = 0.43 - 0.3 \times 10^{-2} T + 0.47 \times 10^{-5} T^2 \quad (\text{C6})$$

R.M.S for these fitting equations is approximately (0.025 %). The coefficients with the operating wavelength of LiNbO₃ as in Table (3).

Then the fitting the values in the Table (3) to indicate the coefficients (c_0, c_1, c_2) as a function of wavelength as follow:

$$c_0 = 12.45 - 21\lambda + 8.76\lambda^2 \quad (\text{C7})$$

$$c_1 = -0.97 + 0.16\lambda - 0.067\lambda^2 \quad (\text{C8})$$

$$c_2 = 0.16 \times 10^{-3} - 0.3\lambda + 0.12 \times 10^{-3} \lambda^2 \quad (C9)$$

REFERENCES

- Amersfoort MR, Soole JBD, Leblanc HP, Andreakakis NC, Rajhel A, Caneau C (1996). "Passband Broadening of Integrated Arrayed Waveguide Filters Using Multimode Interference Couplers," *Electron. Lett.* 32(5): 449–451.
- De Peralta LG, Bernussi AA, Gorbounov V, Temkin H (2004). "Temperature-Insensitive Reflective Arrayed Waveguide Grating Multiplexers," *IEEE Photon. Technol. Lett.* 16(3): 831–833.
- Fleming W (1985). "Dispersion in GeO₂-SiO₂ Glasses," *Appl. Opt.* 23(24): 4486–4493.
- Goodman JW (1998). "Introduction to Fourier optics," in *Classic Textbook Reissue Series*. New York: McGraw-Hill, Ch. 5: 83–90.
- Hibino Y (2002). "Recent Advances in High Density and Large Scale AWG Multi/Demultiplexers With Higher Index-Contrast Silica -Based PLCs," *IEEE J. Selected Topics Quantum Elect.* 8 (6): 1090-1101.
- Ho YP, Chen YJ (1997). "Flat Channel-Passband-Wavelength Multiplexing and Demultiplexing Devices by Multiple-Rowland-Circle Design," *IEEE Photon. Technol. Lett.* 9(4): 342-344.
- Ishigure T, Nihei E, Koike Y (1996). "Optimum Refractive Index Profile of The Grade-Index Polymer Optical Fiber, Toward Gigabit Data Link," *Appl. Opt.* 35(12): 2048-2053.
- Jundt DH, (1997). "Fabrication Techniques of Lithium Niobate Waveguides," *Opt. Lett.* 22(9): 1553.
- Kaneko A, Kamei S, Inoue Y, Takahashi H, Sugita A (2000). "A thermal Silica-Based Arrayed-Waveguide Grating (AWG) Multi/Demultiplexer With New Low Loss Groove Design," *Electron. Lett.*, 36(4): 318–319.
- Kang ES, Park JU, Bae BS (2003). "Effect of Organic Modifiers on the Thermo-Optic Characteristics of Inorganic-Organic Hybrid Material Films," *J. Mater. Res.* 18(8): 1889–1894.
- Kato K, Okada A, Sakai Y, Noguchi K, Sakamoto T, Suzuki S, Takahara A, Kamei S, Kaneko A, Matsuoka M (2000). "32 x 32 Full-Mesh (1024 path) Wavelength Routing WDM Optical Access Network Based on Uniform Loss Cyclic-Frequency Arrayed-Waveguide Grating," *IEE Electron. Lett.* 36(15): 1294–1295.
- Kikuchi N, Shibata Y, Okamoto H, Kawaguchi Y, Oku S, Kondo Y, Tohmori Y (2004). "Monolithically Integrated 100-Channel WDM Optical Access Channel Selector Employing Low-Crosstalk Arrayed Waveguide Grating (AWG)," *IEEE Photon. Technol. Lett.* 16(11): 2481-2483.
- Kohotoku M, Shibata Y, Yoshikuni Y (2002). "Evaluation of the Rejection Ratio of An MMI-Based Higher Order Mode Filter Using Optical Low-Coherence Reflectometry", *IEEE Photon. Technol. Lett.*, 14(23): 968-970.
- Kohtoku M, Oku S, Kadota Y, Shibata Y, Yoshikuni Y (2000). "Polarisation-Insensitive Semiconductor Arrayed Waveguide Grating Integrated With Spot Size Converter", *El. Lett.* 36(12): 1055-1056.
- McGreer KA (1998). "Arrayed Waveguide Gratings for Wavelength Routing," *IEEE Commun. Mag.*, 36(4): 62–68.
- Moerman I, Van DPP, Demeester PM (1997). "A technical Review On the Fabrication Technologies For the Monolithic Integration of Optical Tapers with the III-V Semiconductor Materials Optical Devices", *IEEE J. Sel. Topics in Quantum Electron.*, 3(33): 1308 – 1320.
- Noguchi K, Koike Y, Tanobe H, Harada K, Matsuoka M (2004). "Field Trial of Full-Mesh WDM Network (AWG-STAR) in Metropolitan/Local Area," *IEEE J. Lightwave Technol.*, 22(2): 329-336.
- Okamoto K, Hasegawa T, Ishida O, Himeno A, Ohmori Y (1997). "32x32 Arrayed-Waveguide Grating (AWG) Multiplexer with Uniform Loss and Optical Cyclic Frequency Characteristics," *IEE Electron. Lett.*, 33(22): 1865–1866.
- Okamoto K, Sugita A (1996) "Flat Spectral Response Arrayed-Waveguide Grating Multiplexer With Parabolic Waveguides Horns," *Electron Lett.* 32 (16): 1661-1662.
- Okamoto K, Yamada H (1995). "Arrayed-Waveguide Grating Multiplexer with Flat Spectral Response," *Opt. Lett.*, 20(10): 43-45.
- Ooba N, Hibino Y, Inoue Y, Sugita A (2000). "A thermal Silica-Based Arrayed-Waveguide Grating Multiplexer using Bimetal Plate Temperature Compensator," *Electron. Lett.* 36(3): 1800–1801.
- Parker MC, Walker SD (1999). "Design of Arrayed-Waveguide Gratings using Hybrid Fourier-Fresnel Transform Techniques," *IEEE J. Select. Topics Quantum Electron.*, 5(3): 1379–1384.
- Saito T, Nar K, Nekado Y, Hasegawa J, Kashihara KB (2003). "100 GHz-32 Ch A thermal AWG With Extremely Low Temperature Dependency of Center Wavelength," in *Proc. OFC' 03*: 57–59.
- Yong L, Louzhen F (2003). "Comb Wavelength Division Multiplexer," U.S. patent US6 pp. 608-719.